



# Magnesium Application Promotes Rubisco Activation and Contributes to High-Temperature Stress Alleviation in Wheat During the Grain Filling

Yuhang Shao<sup>1</sup>, Shiyu Li<sup>1</sup>, Lijun Gao<sup>1</sup>, Chuanjiao Sun<sup>1</sup>, Jinling Hu<sup>1</sup>, Attiq Ullah<sup>1</sup>, Jingwen Gao<sup>1</sup>, Xinxin Li<sup>2</sup>, Sixi Liu<sup>1,3</sup>, Dong Jiang<sup>1</sup>, Weixing Cao<sup>1</sup>, Zhongwei Tian<sup>1\*</sup> and Tingbo Dai<sup>1\*</sup>

## OPEN ACCESS

### Edited by:

Milton Lima Neto,  
São Paulo State University, Brazil

### Reviewed by:

Ana Karla M. Lobo,  
São Paulo State University, Brazil  
Aurenivia Bonifacio,  
Federal University of Piauí, Brazil  
Marcio Martins,  
Universidade Federal do Acre, Brazil  
Gustaf E. Degen,  
The University of Sheffield,  
United Kingdom

### \*Correspondence:

Tingbo Dai  
tingbod@njau.edu.cn  
Zhongwei Tian  
zhwtian@njau.edu.cn

### Specialty section:

This article was submitted to  
Plant Physiology,  
a section of the journal  
Frontiers in Plant Science

Received: 03 March 2021

Accepted: 21 April 2021

Published: 11 June 2021

### Citation:

Shao Y, Li S, Gao L, Sun C, Hu J, Ullah A, Gao J, Li X, Liu S, Jiang D, Cao W, Tian Z and Dai T (2021) Magnesium Application Promotes Rubisco Activation and Contributes to High-Temperature Stress Alleviation in Wheat During the Grain Filling. *Front. Plant Sci.* 12:675582. doi: 10.3389/fpls.2021.675582

<sup>1</sup> Key Laboratory of Crop Physiology Ecology and Production Management, Ministry of Agriculture and Rural Affairs, Nanjing Agricultural University, Nanjing, China, <sup>2</sup> Rural Energy and Environment Agency, Ministry of Agriculture and Rural Affairs, Beijing, China, <sup>3</sup> Chengdu Agricultural Technology Extension Station, Chengdu, China

Inhibited photosynthesis caused by post-anthesis high-temperature stress (HTS) leads to decreased wheat grain yield. Magnesium (Mg) plays critical roles in photosynthesis; however, its function under HTS during wheat grain filling remains poorly understood. Therefore, in this study, we investigated the effects of Mg on the impact of HTS on photosynthesis during wheat grain filling by conducting pot experiments in controlled-climate chambers. Plants were subjected to a day/night temperature cycle of 32°C/22°C for 5 days during post-anthesis; the control temperature was set at 26°C/16°C. Mg was applied at the booting stage, with untreated plants used as a control. HTS reduced the yield and net photosynthetic rate ( $P_n$ ) of wheat plants. The maximum carboxylation rate ( $V_{Cmax}$ ), which is limited by Rubisco activity, decreased earlier than the light-saturated potential electron transport rate. This decrease in  $V_{Cmax}$  was caused by decreased Rubisco activation state under HTS. Mg application reduced yield loss by stabilizing  $P_n$ . Rubisco activation was enhanced by increasing Rubisco activase activity following Mg application, thereby stabilizing  $P_n$ . We conclude that Mg maintains Rubisco activation, thereby helping to stabilize  $P_n$  under HTS.

**Keywords:** wheat, high-temperature stress, magnesium, Rubisco activity, Rubisco activation, photosynthetic rate, high-temperature stress, photosynthetic rate

## INTRODUCTION

Wheat is a C3 crop that grows during the winter and spring seasons, with an optimum grain filling temperature of 20–24°C (Paulsen, 1994; Shah and Paulsen, 2003; Li et al., 2012). The temperature threshold for grain filling in winter wheat is 25°C (Porter and Gawith, 1999; Wahid et al., 2007). When day/night temperatures increase to 30°C/25°C, the filling duration is shortened and dry matter accumulation decreases (Huebner and Bietz, 1988; Khan et al., 2020). However, the temperature often rises above 30°C in late spring, during the middle or late grain filling late stage, around the middle to lower reaches of the Yangtze River (World Weather Information Service). Grain yield can decrease by up to 30% at temperatures exceeding 32°C

(Al-Khatib and Paulsen, 1990; Djanaguiraman et al., 2020). Global warming has increased the occurrence of intense high-temperature events (IPCC, 2020); as a result, high-temperature stress (HTS) on winter wheat during the grain filling stages restricts wheat production (Lesk et al., 2016).

Under favorable conditions, approximately 70–90% of the final grain yield is obtained from photosynthates produced during grain filling (Austin et al., 1977; Makunga et al., 1978; Chaudhuri et al., 2017). Longer leafing duration and higher photosynthetic activity contribute to yield increases in most major crops (Richards, 2000). However, high temperatures during post-anthesis restrict grain yield by reducing grain filling time and photosynthesis efficiency (Farooq et al., 2011). Photosynthesis is the basis of biomass production and is the physiological process that is most sensitive to elevated temperature, often showing inhibition before all other cellular functions at high temperatures (Berry and Bjorkman, 1980). Several photosynthetic pigment components of photosystem II (PSII), Rubisco carboxylation activity, stomatal opening, and other associated processes, are highly susceptible to HTS (Mathur et al., 2014). Damage to any of these components and processes is sufficient to interrupt the general photosynthetic mechanism (Ashraf and Harris, 2013; Mathur et al., 2014). However, the effects of HTS on the photosynthesis process during the wheat post-anthesis stage remain further understood.

Many studies have suggested that the loss of Rubisco activation is the main factor limiting the net photosynthesis rate under moderate HTS (Demirevska-Kepova and Feller, 2004; Salvucci and Crafts-Brandner, 2004b). Rubisco catalyzes the assimilation of CO<sub>2</sub> during photosynthesis, and its catalytic limitations compromise photosynthesis efficiency (Parry et al., 2008; Lobo et al., 2019). Rubisco binds easily with inhibitors that block its active sites (Parry et al., 2008; Lobo et al., 2019). Rubisco activation state is defined as the fraction of active sites with catalytic activity and is regulated by Rubisco activase (RCA) (Boexfontvieille et al., 2014; Scafaro et al., 2016; Perdomo et al., 2017). Phosphate inhibitors can be removed from Rubisco active sites (carbamylation or not) via RCA activity in an ATP-dependent reaction (Streusand and Portis, 1987; Bracher et al., 2017). Under HTS, when Rubisco deactivation speeds up and photosynthesis is inhibited, the role of RCA becomes increasingly evident (Portis, 2003; Ristic et al., 2009; Scafaro et al., 2016; Perdomo et al., 2017). RCA is extremely sensitive to temperature (Kurek et al., 2007), but thermally stable RCA maintains high Rubisco activation levels and increases CO<sub>2</sub> fixation efficiency (Kurek et al., 2007; Scafaro et al., 2016, 2019; Shivhare and Mueller-Cajar, 2017; Degen et al., 2020, 2021). Thus, improving RCA activity may be an effective method for maintaining a higher photosynthesis rate under HTS.

Magnesium (Mg) is involved in several physiological and biochemical processes of plant growth and development (Waraich et al., 2011). Up to 15–35% of total Mg in plants is located in chloroplasts (Karley and White, 2009; Chen et al., 2018), where it is involved in photophosphorylation and CO<sub>2</sub> fixation (Cakmak and Yazici, 2010). Mg mainly plays roles in Rubisco activation and RCA catalysis (Parry et al., 2008). Mg deficiency adversely affects CO<sub>2</sub> fixation, leading to reduced

photosynthesis rates (Andersson, 2008), whereas adequate Mg has been shown to alleviate adverse effects of HTS in wheat and maize seedlings (Mengutay et al., 2013). Thus, Mg may play a significant part in carbon reactions, representing a possible mechanism for stabilizing the net photosynthesis rate under HTS.

High-temperature stress frequently occurs during the grain filling stage; however, few studies have examined Mg functions involved in photosynthesis under HTS during the grain filling stage. We hypothesized that under HTS, Mg application would enhance Rubisco activation, contributing to HTS alleviation. Therefore, we examined variation in Rubisco content and Rubisco activation state, light energy utilization efficiency under HTS to evaluate the effects of Mg application on Rubisco carboxylation activity, and electron transport capacity under HTS.

## MATERIALS AND METHODS

### Plant Culture and Growth Conditions

We conducted pot experiments at the Pailou Experimental Station of NAU, China (32°04'N, 118°76'E), during the 2016–2018 growing season. The local widely grown cultivar of Yangmai-16 (*Triticum aestivum* L.) was grown in plastic pots with a volume of 0.015 m<sup>3</sup> (height, 30 cm; diameter, 25 cm), each with three holes at the bottom. Every pot was filled with 9 kg of air-dried and uniformly mixed clayey loam soil sieved through a 0.5-mm mesh. The soil contained 11.78 g kg<sup>-1</sup> organic matter, 0.87 g kg<sup>-1</sup> total nitrogen (N), 81.37 mg kg<sup>-1</sup> available potassium (K), 19.25 mg kg<sup>-1</sup> available phosphate (P), and 110.9 mg kg<sup>-1</sup> available Mg. After soil filling, 5 g of compound fertilizer (15% N, 15% P, and 15% K) was applied to each treatment. At the jointing (Feekes 6.0) and booting stages (Feekes 10.0) (Miller, 1992), 0.45 g of N was applied to each pot. Each pot was sowed with 18 seeds, and then seedlings were scattered to eight in each pot at the three-leaf stage.

### Treatment Application and Management

Magnesium fertilizer in the form of MgSO<sub>4</sub>·7H<sub>2</sub>O was applied at 0.85 g per pot (0.11 g·kg<sup>-1</sup>) at the booting stage (Feekes 10.0), and pots without additional Mg application were used as controls (CK). The pots were moved to climate-controlled chambers set at a different temperature for 16–20 days after anthesis (DAA). HTS of the air temperature was simulated at 32°C/22°C, and 26°C/16°C was applied as the optimal temperature (OT). The temperature setting during treatment days and the leaf temperature are shown in **Supplementary Figure 1**. Relative humidity in the chambers was at 65%, under a light intensity of 1500 μmol photons m<sup>-2</sup> s<sup>-1</sup> with a photoperiod of 16 h. Each pot was watered about 2–4 l each morning and evening during post-anthesis. Following treatment, pots were relocated in the OT growth chamber until maturity. Thus, the four treatments were CK-OT (control fertilizer with optimal temperature), CK-HT (control fertilizer with HTS), Mg-OT (additional Mg fertilizer with optimal temperature), and Mg-HT (additional Mg fertilizer with HTS).

## Plant Sampling and Measurements

Plant sampling were conducted at 15DAA (prior to HTS treatment), 17DAA (2 days after treatment), 20DAA (5 days after treatment), and 25DAA. The flag leaves were detached from five randomly selected pots for each treatment and immediately submerged in liquid nitrogen for fresh sample measurements. Dry samples were collected from whole plants in five randomly selected pots of each treatment. We manually cut the plants at ground level using pruning scissors and then dried the samples at 105°C for 15 min in the oven, followed by 70°C until constant weight. The dried samples were ground for N and Mg content determination. Yield measurements at the maturity stage were tracked using the same five pots in each treatment.

## Gas Exchange and Fluorescence Measurements

### Gas Exchange Measurements

The gas exchange parameters were measured in flag leaves using the red and blue light source chamber (LI6400-02B) of a gas exchange machine (Li-Cor 6400, Li-Cor Inc., United States) in this study. The gas exchange parameter measurements were according to the methods by Gao et al. (2018) with modifications. Measurements were performed from 9:00 to 11:00 am under a light level of 1500  $\mu\text{mol photons m}^{-2} \text{s}^{-1}$ . The vapor pressure deficit was between 0.5 and 1.0 kPa. The reference  $\text{CO}_2$  concentration level was set at 400  $\mu\text{mol mol}^{-1}$ , and the relative humidity of the leaf chamber was set to 55–65%. The temperature of the leaf chamber was set according to real-time temperature in the growth chamber. The equipment was preheated for 0.5 h prior to measurement, and data were recorded three times after cuvette acclimatization for at least 5 min.

The net photosynthesis rate/intercellular  $\text{CO}_2$  concentration ( $A-C_i$ ) curve was determined according to Gao et al. (2018). Measurements were conducted using the red and blue light source chamber of the Li-Cor 6400 photosynthesis instrument. The setting of light level and relative humidity was the same with the previous setting. A  $\text{CO}_2$  injection system was used to control the  $\text{CO}_2$  concentration. Leaves were placed in the chamber for 10 min for adaptation. The  $\text{CO}_2$  concentration in the leaf chamber was then adjusted to values of 400, 200, 100, 50, 100, 150, 200, 400, 600, 800, 1000, 1200, and 1600  $\mu\text{mol mol}^{-1}$ , and data were recorded for about 3 min per setting. Plotting  $P_n$  as the vertical coordinate and  $C_i$  as horizontal coordinate, the initial slope of the curve ( $C_i < 200 \mu\text{mol mol}^{-1}$ ) represented carboxylation efficiency (CE). The Rubisco maximum carboxylation rate ( $V_{Cmax}$ ) and maximum electron transport rate ( $J_{max}$ ) were calculated according to modified equations (Long and Bernacchi, 2003; Li et al., 2009; Gao et al., 2018). The  $A-C_i$  curve is shown in the **Supplementary Figure 2**.

### Chlorophyll Fluorescence Measurements

The fluorescence parameters were determined using the machine of CF Imager, Technologia Ltd, Colchester, United Kingdom. Following the methods of Gao et al. (2018), we selected leaves that had been adapted to the light for more than 30 min and recorded the steady-state fluorescence ( $F_s$ ) and then applied a

flash ( $\sim 8000 \mu\text{mol photons m}^{-2} \text{s}^{-1}$ ) to record the maximum fluorescence under light ( $F_m'$ ). We maintained the leaves in the dark for 3 s, turned on the far-red light, then measured the initial fluorescence  $F_o'$  under the light. Next, the leaves were shaded and dark-adapted for more than 30 min, and the minimum ( $F_o$ ) and maximum ( $F_m$ ) chlorophyll fluorescence were recorded. Then, we calculated PSII efficiency ( $\Phi_{PSII}$ ) as  $\Phi_{PSII} = (F_m' - F_s)/F_m'$ , maximum fluorescence as  $F_m = F_m' - F_o/F_m'$  (Genty et al., 1989), photoinhibitory quenching (qL) as  $qL = F_o'/F_s \times (F_m' - F_s)/(F_m' - F_o')$  (Kramer et al., 2004), and the electron transport rate (ETR) as  $ETR = (F_m' - F_s)/F_m' \times \text{PPFD} \times 0.85 \times 0.5$  (Li et al., 2009).

## Physiological Measurements and Chemical Analysis

### N and Mg Content Determination

We used 100 mg ground dried samples to determine Mg content. The samples were extracted using 5 mL of  $\text{HNO}_3$  and HCl solution (1:1 v/v) for 4 h at 50°C, and then the volume was adjusted to 20 mL using ddH<sub>2</sub>O. Five biological repeats were conducted separately. Mg content was analyzed using the ICP-OES, Optima 8000.

Total N analyses were conducted with the method from micro-Kjeldahl (Santos and Boiteux, 2013). Dried samples (0.2 g) from flag leaves were used. Five biological repeats were performed independently.

### Chlorophyll Content Measurements

Chlorophyll concentrations were measured spectrophotometrically according to Arnon (1949). We used 0.05 g of fresh flag leaves and 25 mL of a mixture of acetone and absolute ethanol (volume ratio 1:1) to extract leaf pigments. The samples were placed in a 30°C incubator for about 24 h, and the extract was mixed several times. The absorbances at 470, 645, and 663 nm were measured to calculate the Chl a and Chl b concentrations, respectively. The chlorophyll concentration is the sum of Chl a and Chl b.

### Rubisco and Rubisco Activase (RCA) Content Determination

Rubisco content was measured using SDS-PAGE following the methods of Makino et al. (1985) with modifications. We ground 10-cm<sup>2</sup> frozen leaf samples and extracted each sample in 5 mL of buffer solution prepared according to the methods. Then, we centrifuge the mixture at 15,000  $\times g$  for 15 min at 4°C and mixed the crude enzymatic extract with 5  $\times$  loading buffer. We boiled 1 mL of the mixture for 1 min prior to electrophoresis. The amount of each sample was 10  $\mu\text{L}$  used in the electrophoresis which was at 100 V for about 8 h. After that, the gels were stained with 0.25% (w/v) Coomassie Blue R-250. The gels were destained with 25% ethanol and 8% glacial acetic acid solution. Subunits of 55 and 15 kDa were put into a container with 2 mL of formamide. Then, the samples were kept in a 50°C water bath overnight. The absorbance at 595 nm ( $\text{OD}_{595}$ ) was measured. The calibration curve is shown in the **Supplementary Figure 3**.

Rubisco activase content was determined using an RCA Kit [Plant Rubisco Activase Enzyme-linked Immunoassay Assay (ELISA) Kit, Jianglai Biotechnology Co., Ltd., Shanghai]

according to the manufacturer's instructions. The double-antibody sandwich method was used to determine the RCA content of the plant according to Choi and Roh (2003) with modifications. Ten microliters of crude enzymatic extract with 40  $\mu\text{L}$  sample diluent was added with 100  $\mu\text{L}$  of rabbit anti-Rubisco activase antiserum in a 96-well microtiter plate, which were precoated with the RCA capture antibody. Then, the plate was incubated at 37°C for 60 min. After washing the plate five times, 100  $\mu\text{L}$  peroxidase substrate was added. After mixing, the plate was kept in the dark for 15 min at room temperature. Finally, 1 M HCl was added to terminate the reaction. We measured OD<sub>450</sub> within 15 min after adding the termination solution.

### Rubisco and RCA Activity Determination

Rubisco activity was determined following the method of Sharwood et al. (2016). We measured the rate of NADH oxidation at 340 nm. The NADH-linked assays retrieve lower values of Rubisco activity compared with the <sup>14</sup>CO<sub>2</sub> fixation assay, but the NADH-linked assays were correlated strongly with the radiometric assay (Sales et al., 2020). NADH-linked assay is widely used in Rubisco activity, but microtiter plate-based assays may decrease the accuracy of the results (Sales et al., 2020), so we utilized cuvettes to measure the change in absorbance in a spectrophotometer. The recipes of extract buffer solution [5 ml pH 8.0 buffer solution (50 mM pH 7.5 Tris-HCl), 10 mM  $\beta$ -mercaptoethanol, 12.5% (v/v glycerol, 1 mM EDTA-Na<sub>2</sub>, 10 mM MgCl<sub>2</sub>, 1% (m/v) polyvinylpyrrolidone)], assay buffer solution (100 mmol EPPS-NaOH pH 8.0, 10 mmol MgCl<sub>2</sub>, 1 mmol EDTA, 0.2 mmol NADH, 20 mmol NaHCO<sub>3</sub>, 5 mmol dithiothreitol, 5 mmol ATP, 10 U·ml<sup>-1</sup> creatine phosphokinase, 10 U·ml<sup>-1</sup> 3-phosphoglyceric phosphokinases, 10 U·ml<sup>-1</sup> glyceraldehyde-3-phosphate dehydrogenases, and 5 mmol phosphocreatine), and activating solution (50 mM Tris-HCl pH 7.5, 40 mM MgCl<sub>2</sub>, 20 mM NaHCO<sub>3</sub>) were according to Gao et al. (2018). We ground 10-cm<sup>2</sup> frozen leaf samples and extracted each sample using 5 mL of pH 8.0 buffer solution. The mixture was centrifuged at 15,000  $\times$  g for 1 min at 4°C. The initial Rubisco activity was measured using a cuvette containing 100  $\mu\text{L}$  of the crude enzymatic extract, 700  $\mu\text{L}$  of assay buffer, and 200  $\mu\text{L}$  of 10 mmol RuBP. The change in absorbance at 340 nm was monitored for 60 s (3 s per measurement) at room temperature. To determine the total Rubisco activity, 100  $\mu\text{L}$  of crude enzymatic extract was activated for 10 min at 25°C in RuBP assay buffer by adding 100  $\mu\text{L}$  of activating solution. Next, 100  $\mu\text{L}$  of this mixture was added with 700  $\mu\text{L}$  of assay buffer and 200  $\mu\text{L}$  of 10 mmol RuBP sequentially, and the OD value at 340 nm was monitored for 1 min (3 s per measurement). The ratio of the initial activity over the total activity was calculated as the Rubisco activation state.

Rubisco activase activity measurements were processed following the process from Carmo-Silva and Salvucci (2011). The uncarbamylation of Rubisco in the desalt extracts promoted the formation of the inactive Rubisco-RuBP complex. Frozen leaves were rapidly extracted at 4°C with 5% PEG<sub>3350</sub> and 4 mM RuBP and then incubated for 5 min at 4°C. Next, the extract was added to two parallel (A and B) reactions at 25°C. The recipes of the A and B solutions were according to

Carmo-Silva and Salvucci (2011). In these reactions, the RuBP concentration was 3.6 mM. Rubisco activation was tracked by evaluating Rubisco activity in aliquots taken at every half minute till 5 min after initiation of reaction. The rate of Rubisco activity was the increase in the fraction of Rubisco active sites from 1.5 to 3 min by determining the Rubisco activity in reactions without ATP.

### ATP and ADP Content Determination

We used ATP and ADP Bioluminescence Assay Kit (Beyotime, Jiangsu, China) to determine ATP and ADP contents, respectively, following the manufacturer's instructions. Twenty milligrams of wheat leaf samples were collected in 200  $\mu\text{L}$  pre-chilled lysis buffer, and a glass homogenizer was used to fully lyse the leaf tissue. The samples were centrifuged at 10,000  $\times$  g for 2 min at 4°C. The supernatant was collected. The ATP detection working solution was prepared according to the kit protocol. To each well, we added 100  $\mu\text{L}$  of extract, followed by 100  $\mu\text{L}$  of working solution. The luciferase signals were detected for 30 s using a multifunctional microplate reader (SpectraMax M2). A standard ATP concentration curve ranging from 1 pM to 1 M was prepared by gradient dilution. ADP concentration measurements were conducted by conversion to ATP.

### Statistical Analysis

All data were analyzed using the SPSS ver. 10.0 software (SPSS Inc., United States). Two-way analysis of variance was performed for all data, and the means were compared using Duncan's multiple-comparison tests at a significance level of  $P < 0.05$ . We used a minimum of three biological replicates. All graphs presented were produced using the GraphPad Prism 9 (GraphPad Software, San Diego, CA, United States), and tables were produced using Microsoft Excel 2016 (Microsoft, Redmond, WA, United States).

## RESULTS AND DISCUSSION

### Results

#### Grain Filling Duration, Biomass, and Yield

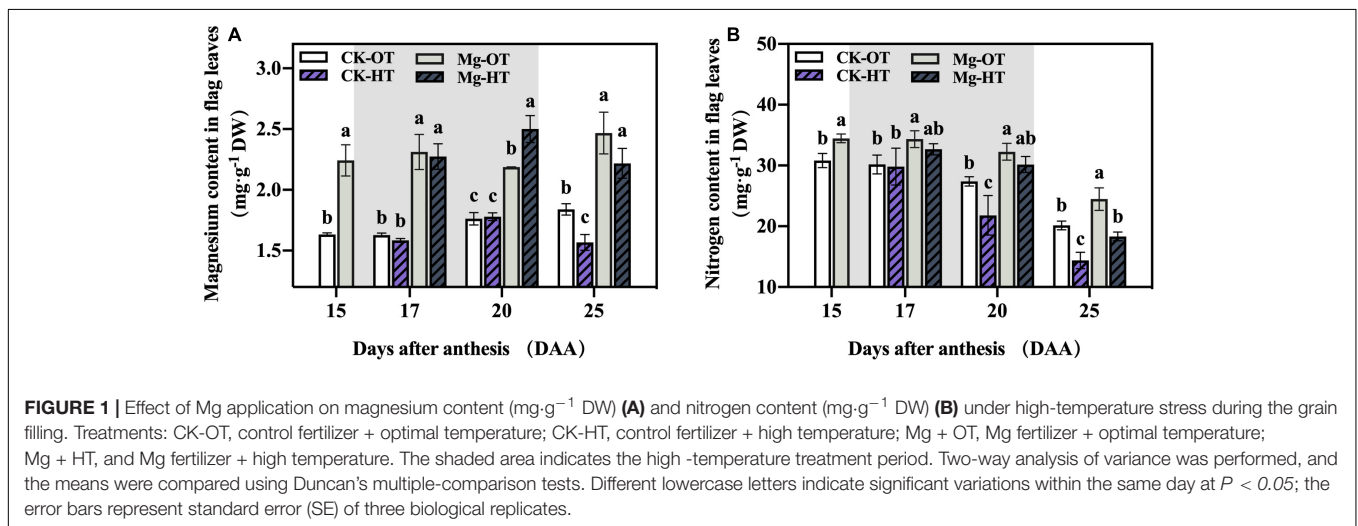
High-temperature stress treatment significantly affected the 1000-grain weight of wheat plants, resulting in decreased yield (Table 1). The 1000-grain weight was reduced by 8.37 and 8.48% in the CK-HT treatment and by 5.01 and 5.51% in the Mg-HT treatment, during 2016–2017 and 2017–2018, respectively. Grain yield was reduced by 10.28 and 10.89% in the CK-HT treatment and by 6.6 and 7.9% in the Mg-HT treatment during 2016–2017 and 2017–2018, respectively. Mg treatment reduced the loss in grain weight and yield caused by HTS.

After anthesis, CK-HT and Mg-HT treatment durations were shortened by about 3 days due to HTS (Table 1). However, the duration of Mg-OT treatment was prolonged by about 3 days compared to CK-OT. As a result of HTS, biomass accumulation after anthesis declined more in CK-HT (12.91 and 16.12%, 2016–2017 and 2017–2018, respectively) than in Mg-HT treatment (8.03 and 7.92%) (Table 1). Biomass at maturity decreased under HTS treatment by 4.48 and 5.75% in CK-HT, and 2.94 and

**TABLE 1** | Effect of Mg application on the grain filling duration (days), post-anthesis biomass (PAB, g pot<sup>-1</sup>), biomass at maturity (MB), 1000-kernel weight (TKW, g), and grain yield (g pot<sup>-1</sup>) of wheat under high-temperature stress (HTS) during grain filling.

	Treatments	Filling duration	PAB	MB	TKW	Grain yield
2016–2017	CK-OT	34.67 <sup>ab</sup>	33.71 <sup>b</sup>	108.5 <sup>b</sup>	41.20 <sup>b</sup>	43.48 <sup>b</sup>
	CK-HT	31.33 <sup>c</sup>	27.47 <sup>c</sup>	102.3 <sup>c</sup>	37.75 <sup>c</sup>	39.01 <sup>c</sup>
	Mg-OT	36.33 <sup>a</sup>	36.11 <sup>a</sup>	112.6 <sup>a</sup>	44.43 <sup>a</sup>	47.42 <sup>a</sup>
	Mg-HT	34.00 <sup>b</sup>	32.86 <sup>b</sup>	109.3 <sup>b</sup>	42.20 <sup>b</sup>	44.29 <sup>b</sup>
2017–2018	CK-OT	35.33 <sup>ab</sup>	33.50 <sup>b</sup>	111.1 <sup>b</sup>	43.04 <sup>b</sup>	47.56 <sup>b</sup>
	CK-HT	32.00 <sup>c</sup>	28.53 <sup>c</sup>	106.1 <sup>c</sup>	39.39 <sup>c</sup>	42.38 <sup>c</sup>
	Mg-OT	37.33 <sup>a</sup>	37.66 <sup>a</sup>	116.5 <sup>a</sup>	46.28 <sup>a</sup>	51.24 <sup>a</sup>
	Mg-HT	34.33 <sup>b</sup>	34.24 <sup>b</sup>	113.0 <sup>b</sup>	43.73 <sup>b</sup>	47.17 <sup>b</sup>

CK-OT, control fertilizer with optimal temperature (OT); CK-HT, control fertilizer with high-temperature stress (HTS); Mg-OT, Mg with OT; Mg-HT, and Mg with HTS. Means were compared using Duncan's multiple-comparison tests. Different lowercase letters after data in the same column indicate significant variations within the same year at  $P < 0.05$ .



2.89% in the Mg-HT treatment during both years (Table 1). These results indicate that Mg application enhanced biomass accumulation and reduced the loss induced by HTS.

### Mg and N Content

The effects of Mg application on Mg and N content in flag leaves under HTS are shown in Figure 1. Mg application promoted increases in Mg and N content in flag leaves at 15DAA. Mg and N content did not change significantly in plants under HTS (CK-HT) relative to control plants (CK-OT) at 17DAA, but a reduction in N content was observed at 20DAA. At 25DAA, Mg and N contents in flag leaves of CK-HT decreased significantly. However, in Mg-treated plants, the Mg content of flag leaves increased dramatically at 20DAA and decreased at 25DAA in Mg-HT, although these differences were not significant compared to the Mg-OT treatment. The N content of flag leaves remained stable at 20DAA and decreased significantly at 25DAA in Mg-HT plants. These results indicate that Mg treatment increased the Mg and N content of flag leaves and reduced N loss induced by HTS.

### Photosynthesis and Related Attributes

The  $P_n$  of wheat flag leaves under all treatments generally decreased during growth (Figure 2). HTS decreased  $P_n$

(9.93%), transpiration rate ( $T_r$ ) (5.64%), leaf stomatal conductance ( $G_s$ ) (2.64%), and chlorophyll content (3.33%) and increased  $C_i$  (8.84%) at 17DAA, although the changes in  $G_s$ ,  $T_r$ , and chlorophyll contents were not significant. At 20DAA,  $P_n$ ,  $G_s$ ,  $T_r$ , and chlorophyll contents decreased under HTS by 17.89, 9.14, 13.11, and 9.57%, respectively, compared with CK-OT, whereas  $C_i$  increased significantly, by 11.10%. Similar trends were observed at both 25DAA and 30DAA. At 17DAA in the Mg-HT treatment,  $P_n$  (4.30%),  $G_s$  (2.08%),  $T_r$  (4.25%), and chlorophyll contents (2.63%) were decreased and  $C_i$  (2.34%) was increased, but not significantly. At 20DAA, Mg-HT treatment stabilized  $C_i$  (4.91% increase, less than CK-HT), and  $P_n$ ,  $G_s$ ,  $T_r$ , and chlorophyll contents decreased by 9.92, 7.33, 8.55, and 6.10%, respectively, compared to Mg-OT. Plants were also less affected by HTS in the Mg-HT treatment than in the CK-HT treatment at 25DAA and 30DAA. The above results indicated that Mg could enhance the photosynthetic capability and stabilize that under HTS.

HTS decreased CE (27.27%) and  $V_{Cmax}$  (21.71%) at 17DAA in CK-HT and also decreased  $J_{max}$  (5.02%), but not significantly (Table 2). CE,  $V_{Cmax}$ , and  $J_{max}$  decreased significantly at 20DAA and 25DAA. These findings indicate that CE and  $V_{Cmax}$  were

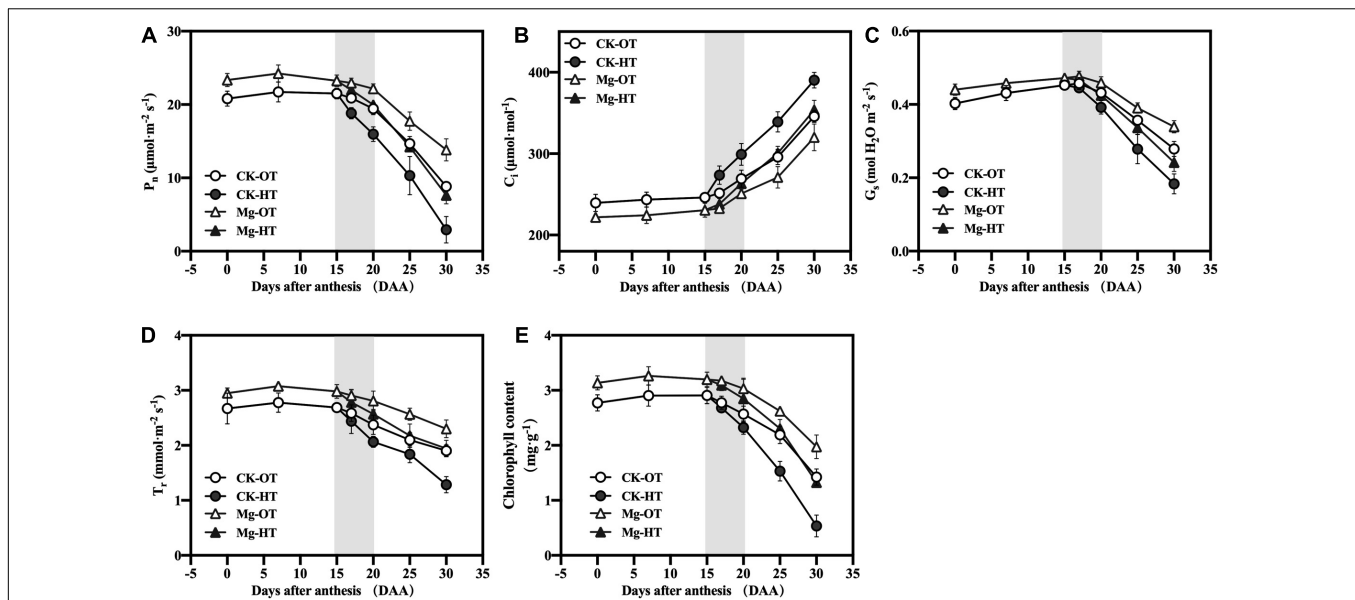


**FIGURE 2 |** Effect of Mg application on net photosynthesis rate ( $P_n$ ) (A), intercellular  $\text{CO}_2$  concentration ( $C_i$ ) (B), stomatal conductance ( $G_s$ ) (C), transpiration rate ( $T_r$ ) (D), and chlorophyll content (E) under high-temperature stress during the grain filling. Vertical bars above mean indicate the SE of five replicates at  $P < 0.5$ .

**TABLE 2 |** Effects of Mg application on carboxylation efficiency (CE), light-saturated potential rate of electron transport ( $J_{max}$ ,  $\mu\text{mol}\cdot\text{m}^{-2}\cdot\text{s}^{-1}$ ), maximum carboxylation rate limited by Rubisco ( $V_{Cmax}$ ,  $\mu\text{mol}\cdot\text{m}^{-2}\cdot\text{s}^{-1}$ ) under HTS during the grain filling stage.

		CE	$V_{Cmax}$	$J_{max}$
15DAA	CK	0.11 <sup>b</sup>	80.93 <sup>b</sup>	170.07 <sup>a</sup>
	Mg	0.14 <sup>a</sup>	91.35 <sup>a</sup>	175.90 <sup>a</sup>
17DAA	CK-OT	0.11 <sup>b</sup>	76.45 <sup>b</sup>	164.87 <sup>ab</sup>
	CK-HT	0.08 <sup>c</sup>	59.85 <sup>c</sup>	156.60 <sup>b</sup>
	Mg-OT	0.13 <sup>a</sup>	89.82 <sup>a</sup>	170.96 <sup>a</sup>
	Mg-HT	0.13 <sup>a</sup>	82.74 <sup>ab</sup>	165.88 <sup>ab</sup>
20DAA	CK-OT	0.10 <sup>b</sup>	67.24 <sup>b</sup>	153.27 <sup>a</sup>
	CK-HT	0.07 <sup>c</sup>	51.03 <sup>c</sup>	129.81 <sup>c</sup>
	Mg-OT	0.13 <sup>a</sup>	79.96 <sup>a</sup>	159.73 <sup>a</sup>
	Mg-HT	0.09 <sup>b</sup>	69.82 <sup>b</sup>	141.66 <sup>b</sup>
25DAA	CK-OT	0.07 <sup>b</sup>	55.10 <sup>b</sup>	137.26 <sup>a</sup>
	CK-HT	0.03 <sup>c</sup>	38.87 <sup>c</sup>	87.03 <sup>c</sup>
	Mg-OT	0.10 <sup>a</sup>	68.89 <sup>a</sup>	143.26 <sup>a</sup>
	Mg-HT	0.06 <sup>b</sup>	57.93 <sup>b</sup>	105.57 <sup>b</sup>

Means were compared using Duncan's multiple-comparison tests. Different lowercase letters after data in the same column indicate significant variations within the same year at  $P < 0.05$ .

inhibited earlier than  $J_{max}$  under HTS. At 15DAA, Mg application improved CE and  $V_{Cmax}$ . Moreover, compared with CK-HT,  $V_{Cmax}$  and CE did not change significantly following Mg treatment at 17DAA under HTS. At 20DAA and 25DAA, CE,  $V_{Cmax}$ , and  $J_{max}$  remained at higher levels in the Mg treatment than in CK. The difference responses between CK-HT and Mg-HT at 17DAA suggested the Mg function in the photosynthesis process under HTS.

### Light Energy Utilization and ETR

Light-dependent reactions showed that HTS did not decrease the maximum photochemical efficiency ( $F_v/F_m$ ) at 17DAA, but  $\Phi_{PSII}$  and ETR decreased due to a reduction in qL in the CK-HT treatment (Table 3). Higher non-photochemical chlorophyll fluorescence quenching (NPQ) was observed in CK-HT at 17DAA.  $\Phi_{PSII}$ , qL,  $F_v/F_m$ , and ETR decreased significantly at 20DAA and 25DAA, and NPQ increased. Mg-treated plants showed significantly higher  $\Phi_{PSII}$ , qL, and ETR at 15DAA, which was consistent with  $P_n$  and its attributes.  $\Phi_{PSII}$ , qL, ETR, and  $F_v/F_m$  were reduced at 20DAA and 25DAA in both CK-HT and Mg-HT, but smaller reductions were observed in Mg-HT plants. A small reduction in NPQ was also observed in Mg-treated plants under HTS. These results indicated that compared with the control, Mg-treated plants had a stronger light energy utilization ability and maintains electron transfer under HTS.

### Rubisco Content and Activation State

Rubisco content and total activity decreased significantly under HTS at 20DAA and 25DAA (Figures 3A,B), but they did not change significantly at 17DAA. HTS led to significantly decreased initial activity at 17DAA, 20DAA, and 25DAA (Figures 3C,D). Mg-OT plants showed higher Rubisco content (Figure 3A), total and initial activity (Figures 3B,C), and activation state (Figure 3D) compared to CK-OT at 15DAA. Rubisco content, total activity, and initial activity were higher in Mg-OT plants than CK-OT at 17DAA, 20DAA, and 25DAA. Interestingly, the initial Rubisco activity and the activation state were maintained in Mg-treated plants relative to CK-HT plants at 17DAA, although decreasing trends were observed in Mg-HT plants at 20DAA and 25DAA.

**TABLE 3 |** Effects of Mg application on actual photochemical efficiency of PSII in the light ( $\Phi_{PSII}$ ), photochemical quenching (qL), the maximum quantum efficiency of PSII ( $F_v/F_m$ ), electron transport rate (ETR), and non-photochemical quenching (NPQ) under HTS during the grain filling stage.

	Treatment	$\Phi_{PSII}$	qL	ETR	NPQ	$F_v/F_m$
DAA15	CK	0.39 <sup>b</sup>	0.33 <sup>b</sup>	131.71 <sup>b</sup>	1.89 <sup>a</sup>	0.82 <sup>ab</sup>
	Mg	0.42 <sup>a</sup>	0.38 <sup>a</sup>	140.22 <sup>a</sup>	1.91 <sup>a</sup>	0.84 <sup>a</sup>
DAA17	CK-OT	0.38 <sup>b</sup>	0.29 <sup>b</sup>	126.22 <sup>b</sup>	1.96 <sup>b</sup>	0.83 <sup>a</sup>
	CK-HT	0.32 <sup>c</sup>	0.24 <sup>c</sup>	107.52 <sup>c</sup>	2.37 <sup>a</sup>	0.82 <sup>ab</sup>
	Mg-OT	0.40 <sup>a</sup>	0.32 <sup>a</sup>	134.18 <sup>a</sup>	1.94 <sup>b</sup>	0.83 <sup>a</sup>
DAA20	Mg-HT	0.39 <sup>a</sup>	0.31 <sup>a</sup>	131.41 <sup>a</sup>	2.05 <sup>b</sup>	0.83 <sup>a</sup>
	CK-OT	0.35 <sup>b</sup>	0.28 <sup>b</sup>	118.33 <sup>b</sup>	2.01 <sup>c</sup>	0.81 <sup>a</sup>
	CK-HT	0.30 <sup>c</sup>	0.22 <sup>c</sup>	100.62 <sup>c</sup>	2.74 <sup>a</sup>	0.76 <sup>c</sup>
DAA25	Mg-OT	0.38 <sup>a</sup>	0.32 <sup>a</sup>	128.10 <sup>a</sup>	2.03 <sup>c</sup>	0.83 <sup>a</sup>
	Mg-HT	0.34 <sup>b</sup>	0.28 <sup>b</sup>	115.08 <sup>b</sup>	2.36 <sup>b</sup>	0.79 <sup>b</sup>
	CK-OT	0.24 <sup>b</sup>	0.26 <sup>b</sup>	79.18 <sup>b</sup>	2.35 <sup>bc</sup>	0.76 <sup>b</sup>
DAA25	CK-HT	0.16 <sup>c</sup>	0.15 <sup>d</sup>	54.99 <sup>c</sup>	3.48 <sup>a</sup>	0.73 <sup>c</sup>
	Mg-OT	0.30 <sup>a</sup>	0.30 <sup>a</sup>	102.14 <sup>a</sup>	2.03 <sup>c</sup>	0.78 <sup>a</sup>
	Mg-HT	0.26 <sup>b</sup>	0.21 <sup>c</sup>	87.14 <sup>b</sup>	2.73 <sup>b</sup>	0.75 <sup>b</sup>

Means were compared using Duncan's multiple-comparison tests. Different lowercase letters after data in the same column indicate significant variations within the same day ( $P < 0.05$ ,  $n = 5$ ).

Mg-HT plants showed a smaller decrease in initial Rubisco activity and activation state than CK-HT plants at 20DAA and 25DAA. This result was consistent with the result in **Table 2**.

### RCA Concentration and Activity

The initial Rubisco activity and activation state depend on RCA activation. In our study, the total RCA pool was measured without distinguishing isoforms. The RCA concentration did not change significantly at 17DAA but decreased significantly in the CK-HT treatment at 20DAA and 25DAA (**Figure 4A**) and in the Mg-HT treatment at 25DAA. This result was consistent with our Rubisco content results. RCA activity in the Mg treatments was significantly higher than in CK at all stages (**Figure 4B**). Interestingly, HTS decreased RCA activity significantly at 17DAA in CK-HT but did not significantly affect that in the Mg-HT treatment. However, RCA activity decreased significantly under HTS in both CK and Mg treatments at 20DAA and 25DAA.

### ATP and ADP Content and ATP/ADP

Mg application increased the ATP content and ATP/ADP ratio compared with CK in the OT treatment (**Figure 5**). However, there was no significant variation in ADP content between CK and Mg. HTS inhibited ATP synthesis, whereas Mg-HT sustained the ATP synthesis and high ATP/ADP ratios. The reduction in the content in ATP corresponded to the electron transfer rate. ATP and ADP content and the ATP/ADP ratio decreased under HTS at 20DAA and did not recover at 25DAA, indicating that the plants had reached senescence at 25DAA. Together, these results indicate that HTS inhibits ATP and ADP production and decreases the ratio of ATP over ADP but that Mg alleviates these losses.

### Correlations Among the Rubisco Activities, RCA Activity, and ATP/ADP Ratio

The initial Rubisco activity and the total Rubisco activity were positively correlated with Rubisco activation state (**Figure 6A**), while the initial activity contributed more to increased Rubisco activation state than to total Rubisco activity. The RCA activity was also positively correlated with the activation state and the ATP/ADP ratio (**Figures 6B,C**). This implied that a higher ATP/ADP ratio was closely related to the enhancement of the RCA activity, and then the activation state was also improved by higher Rubisco initial activity and RCA activity.

## Discussion

### Yield

Global warming is a significant cause of HTS, which poses a serious threat to wheat production in many countries, especially during the reproductive and grain filling phases (Farooq et al., 2011; Khan et al., 2020). Wheat yield reduction under HTS is correlated with fewer spikes and smaller grains (Gibson and Paulsen, 1999; Lesk et al., 2016), whereas grain weight is significantly reduced by high temperatures in the middle and late stages of grain filling (Tahir and Nakata, 2005; Wajid et al., 2018). Assimilate transport from flag leaf to grain is substantially reduced by temperatures above 30°C (Plaut et al., 2004). In this study, HTS shortened the duration of the post-anthesis stage and decreased biomass accumulation (**Table 1**), seed weight, and grain yield. It has been proposed that grain weight was sensitive to the amount of the Mg in the soil (Potarzycki, 2008; Szulc, 2010; Grzebisz, 2013). In this study, the application of Mg fertilizer promoted crop growth and yield formation, which has also been alleviated under HTS. Leaf symptoms in Mg-deficient plants are similar to those of senescent leaves but can be recovered by sufficient Mg application (Uchida, 2000; Tanoi and Kobayashi, 2015). In this study, Mg application extended the duration of the grain filling stage and produced more biomass after anthesis under HTS, leading to higher grain weight and yield formation.

### Mg and N Content

Under normal conditions, Mg content accounts for 0.15–0.35% of the dry weight of vegetative plant parts (Marschner, 1995; Tanoi and Kobayashi, 2015). During early vegetative growth, the critical whole-shoot Mg concentration is 0.1% for wheat (Jones and Wolf, 1991). In this study, Mg-treated plants alleviated yield loss under HTS and increased yield under normal temperature conditions, perhaps because Mg concentrations in the flag leaves of Mg-treated plants were at adequate levels (Mengutay et al., 2013), whereas CK plants were near the threshold of Mg deficiency. The most significant change during senescence is the breakdown of chloroplasts, which account for more than 70% of total N (Bascunan-Godoy et al., 2018). The rate of senescence and the remobilization of leaf N are related to the plant N nutrition status (Hortensteiner and Feller, 2002; Nehe et al., 2020). Previous studies have suggested that Mg application supports N uptake (Peng et al., 2019). Our findings also demonstrated that Mg promotes N accumulation, which were consistent with those of Peng et al. (2019). Additionally, HTS accelerates N degradation in flag leaves, whereas Mg stabilized N content, which suggests

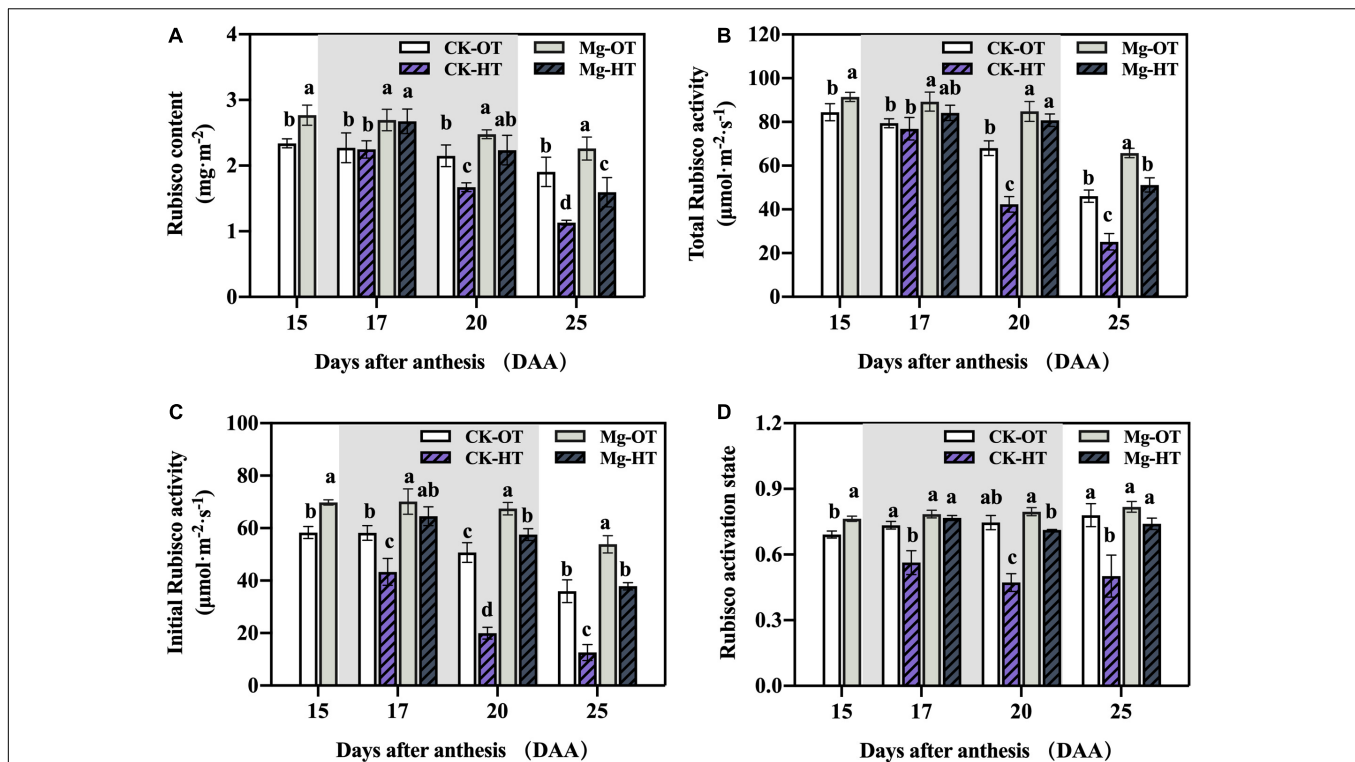


**FIGURE 3 |** Effect of Mg application on Rubisco content and activity under HTS during the grain filling stage. Two-way analysis of variance was performed; each bar is the mean  $\pm$  SE of five replications. Different lowercase letters indicate significant variations within the same day at  $P < 0.5$  (Duncan's multiple-comparison tests). (A) Rubisco content, (B) Total Rubisco activity, (C) Initial Rubisco activity, (D) Rubisco activation state.

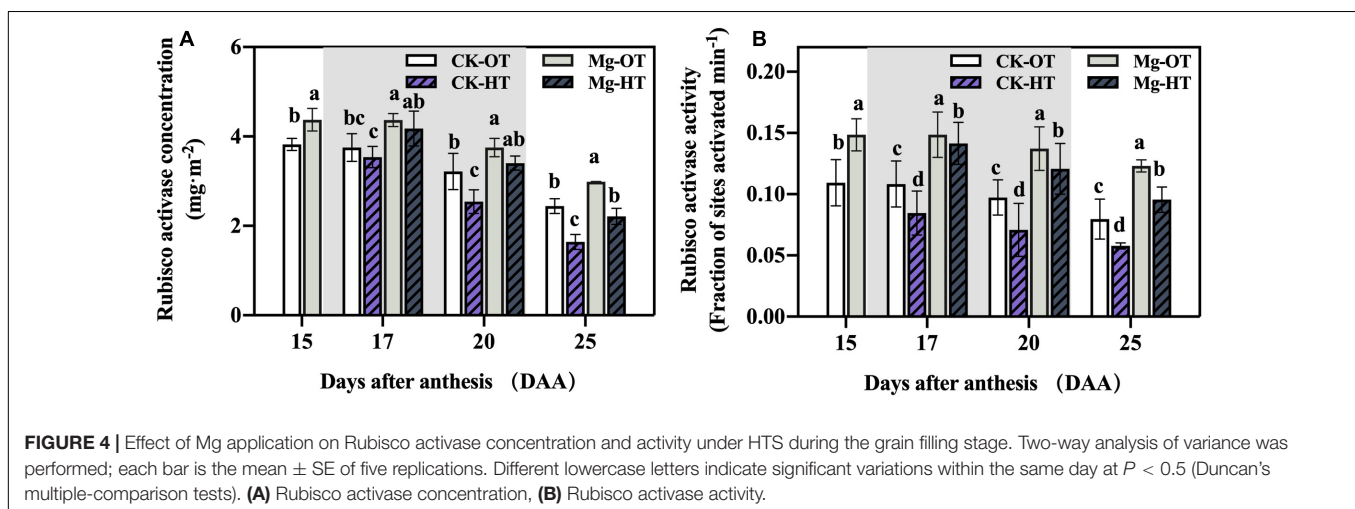


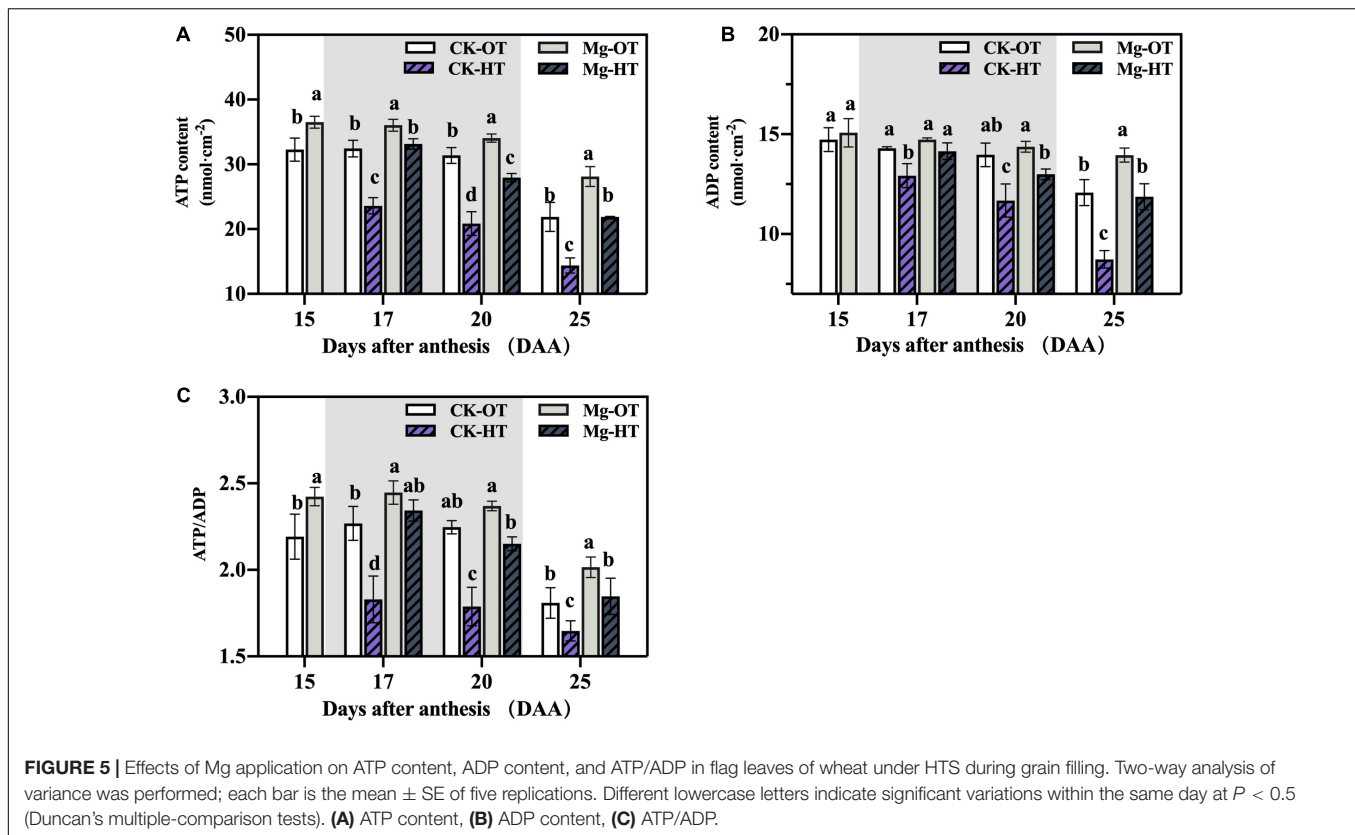
**FIGURE 4 |** Effect of Mg application on Rubisco activase concentration and activity under HTS during the grain filling stage. Two-way analysis of variance was performed; each bar is the mean  $\pm$  SE of five replications. Different lowercase letters indicate significant variations within the same day at  $P < 0.5$  (Duncan's multiple-comparison tests). (A) Rubisco activase concentration, (B) Rubisco activase activity.

that Mg alleviates senescence in flag leaves under HTS during the filling stage.

### Photosynthesis and Related Attributes

Photosynthesis is pivotal to crop yield production, and photosynthetic capacity decreases gradually during plant senescence. Leaf photosynthesis is the physiological process that is most sensitive to HTS (Sabater and Martín, 2013), which significantly affects  $P_n$ ,  $G_s$ ,  $T_r$ , and  $C_i$  (Greer and Weedon, 2012;

Jahan et al., 2019). Reduced  $P_n$  under HTS appears to be caused by non-stomatal factors, because the stomata remain open and  $C_i$  is not reduced when the photosynthetic structure is damaged (Mathur et al., 2014). In this study,  $G_s$  and  $T_r$  were not inhibited, but  $P_n$  decreased at 17DAA, indicating that the reduction in  $P_n$  under HTS in the early stages was not due to stomatal factors. Stabilization of leaf transpiration may be a way for wheat to improve leaf overheating (Yang et al., 2012). However,  $C_i$  increased significantly, indicating that HTS reduced



CO<sub>2</sub> utilization efficiency. Mg treatment improved  $P_n$  prior to HTS treatment.  $P_n$  has been found to be higher in Mg-sufficient plants than in Mg-deficient plants (Laing et al., 2000). In this study,  $P_n$  and  $T_r$  were stabilized in Mg-treated plants at 17DAA under HTS, compared with the CK. Similar Mg effects have been reported in *Torreya grandis* seedlings under toxic lead (Pb<sup>2+</sup>) stress (Shen et al., 2016). Mg application also kept high levels of  $G_s$ , which may be attributed to Mg playing a role in the regulation of anion-cation balance and cell turgor in cells along with K (Gerendás and Führes, 2013; Hasanah, 2018). In this study, photosynthetic capacity gradually decreased with wheat leaf senescence, and its inhibition by HTS was more significant at 25DAA and 30DAA, even in the Mg treatments, indicating that HTS irreversibly accelerates senescence during the grain filling stage in wheat.

The factors directly limiting photosynthesis at different degrees of HTS remain controversial because the photosynthetic system produces varying responses at different temperature ranges (Salvucci and Crafts-Brandner, 2004b; Yamori et al., 2013). CE,  $V_{Cmax}$ , and  $J_{max}$  decreased under HTS (Weston and Bauerle, 2007; Ferguson et al., 2020).  $V_{Cmax}$  decreased earlier than  $J_{max}$  at 17DAA, whereas both decreased synchronously at 20DAA and 25DAA; thus,  $J_{max}$  decreased after  $V_{Cmax}$  inhibition. Under Mg application,  $V_{Cmax}$  did not decrease at 17DAA, indicating that Mg stabilized Rubisco carboxylation capacity under HTS. Even at 20DAA and 25DAA, these levels were higher under Mg treatment; thus, HTS may directly inhibit Rubisco carboxylation activity and electron transfer during the photosynthetic light

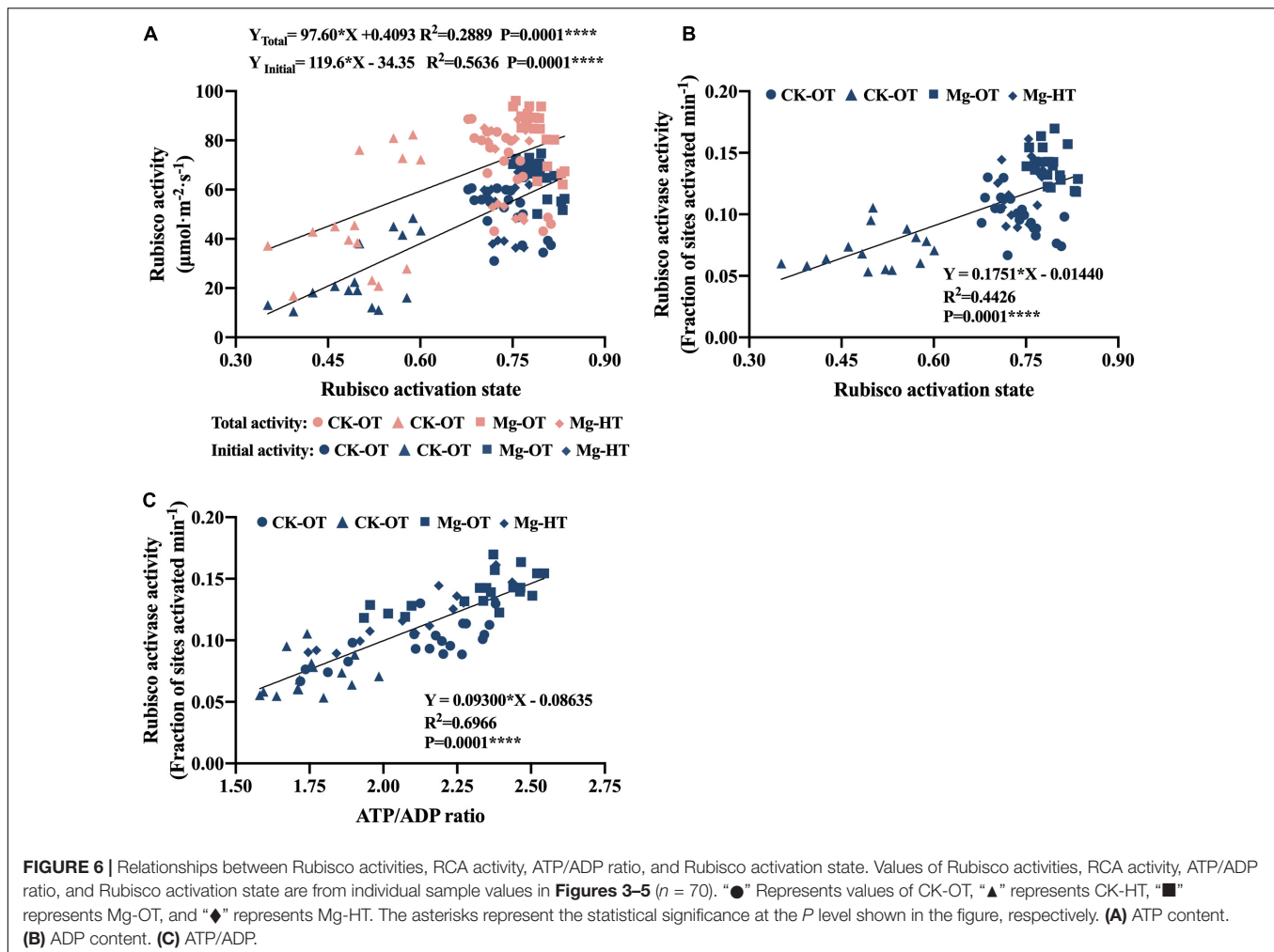
reaction, whereas Mg stabilizes  $V_{Cmax}$  under short-term HTS, promoting carbon reactions.

### Light-Dependent Reaction

The light system of plant leaves absorbs light energy and converts it into ATP and NADPH (Ashraf and Harris, 2013). When these processes are impaired, electron leakage damages the chloroplast structure (Wang et al., 2015).  $F_v/F_m$  is a measure of photosynthetic capacity and can be used to verify the integrity of the PSII (Gregersen et al., 2014). In this study, under short-term HTS (17DAA), the  $F_v/F_m$  of the light reaction system did not change, indicating that the photosynthetic light system of wheat leaves was not damaged under HTS, and the light reaction center retained its ability to self-regulate the photosynthetic system. This finding is consistent with our  $J_{max}$  results. HTS also led to PSII closure in control plants by decreased qL and increased NPQ, which is a strategy for protecting the photosynthetic system under stress conditions (Maxwell and Johnson, 2000). However, PSII remained open in Mg-treated plants under HTS at 17DAA, and higher ETR and  $F_v/F_m$  values were observed at 20DAA and 25DAA, indicating that Mg application under HTS in the grain filling stage promotes light energy utilization and electron transfer, which are beneficial to the synthesis of ATP and NADPH.

### Rubisco Activation

Photosynthesis inhibition in wheat leaves under HTS is mainly caused by decreased Rubisco carboxylation activity



(Scaligero, 2004; Sharwood et al., 2016; Scafaro et al., 2019; Degen et al., 2020, 2021). However, Rubisco is actively degraded during leaf senescence (Imai et al., 2008). In this study, higher Rubisco content was found in Mg-treated plants, which may be related to the uptake of N by applying Mg (Peng et al., 2019), and the Rubisco content is positively correlated with leaf-N content (Makino, 2003). Also, previous studies indicated that total Rubisco activity increased linearly with increasing leaf N (Cheng and Fuchigami, 2000). Therefore, the loss of the total Rubisco activity under HTS at 20DAA and 25DAA may be due to the reduction in the Rubisco amounts caused by accelerated senescence in the flag leaves. Mg stabilized the N content in the leaves, which alleviated the loss of Rubisco amount as well as the total Rubisco activity. However, in this study, under short-term HTS (17DAA), Rubisco content and total activity did not significantly decrease, whereas initial Rubisco activity and activation state were inhibited; this result suggests that Rubisco activation state and activity are sensitive to HTS. Various studies indicated that the decrease in the Rubisco activation state was the main cause of photosynthetic inhibition under moderate heat stress (Salvucci and Crafts-Brandner, 2004a; Degen et al., 2021) and a decrease in the activation state of Rubisco was thought to

reflect a loss of carbamylation due to changes in stromal pH and  $\text{Mg}^{2+}$  concentration (Weis, 1981). In the present study, the initial Rubisco activity decreased earlier at 17DAA and decreased more at 20DAA compared with the total Rubisco activity, which is the reason for the reduction in the Rubisco activation state under HTS. Moreover, previous study has proposed that the decrease in  $\text{Mg}^{2+}$  level in chloroplast caused a significant reduction in Rubisco activity (Lasa et al., 2000). The Rubisco activation obviously depends on the  $\text{Mg}^{2+}$  concentration (Tcherkez, 2013). In the chloroplast, where  $\text{Mg}^{2+}$  total concentration is around 10–20 mM, the RuBP concentration at least twice as high as the concentration in Rubisco sites leads to an activation level of about 90% (Von Caemmere, 1985; Tcherkez, 2013). In our results, Mg treatment significantly increased Rubisco activation state by increasing Rubisco activity, and the Rubisco activation state was stabilized under HTS at 20DAA and 25DAA. Further, in the analysis shown in **Figure 6**, a significant loss of the Rubisco amount caused reductions in the total Rubisco activity at 25DAA, and the initial Rubisco activity decreased significantly at that time. In contrast to previous observations (Perdomo et al., 2017; Degen et al., 2021), Rubisco activation state and Rubisco content were positively correlated, possibly due to the

interplay between heat stress and the onset of leaf senescence. The Rubisco activation state and the total Rubisco activity were decreased synchronously after HTS during the late senescence stage. However, higher initial activity was more closely related to improvements in activation state.

Previous studies have shown that Rubisco enzymes bind easily with sugar phosphate or other substances, which inhibit its function (Parry et al., 2008, 2012; Scafaro et al., 2019; Degen et al., 2020, 2021). RCA and ATP can relieve Rubisco enzyme activity inhibition; therefore, RCA activity is important for stabilizing Rubisco activation (Parry et al., 2008). RCA is directly influenced by temperature (Carmo-Silva and Salvucci, 2012), and it showed the same trend between photosynthetic rate and RCA activity under HTS (Law and Craftsbrandner, 1999). The RCA activity is closely related to the heat tolerance level of wheat (Kumar et al., 2019). In the present study, HTS decreased RCA activity and concentration, but Mg treatment significantly increased RCA activity, which is consistent with the findings of previous studies (Liang et al., 2008; Kuriata et al., 2014; Hazra et al., 2015). Additionally, the RCA activity was also positively correlated with the Rubisco activation state (Figure 6B). Together, our results suggest that Mg promotes RCA activity, thereby stabilizing Rubisco activation under HTS during the wheat grain filling stage.

### Carboxylation and Light-Dependent Reactions Are Interrelated

The CO<sub>2</sub> assimilation reactions (Calvin–Benson cycle) consume ATP and NADPH to regenerate NADP<sup>+</sup> and ADP, reducing the light-dependent reaction and accepting transferred electrons during stable forward photosynthesis (Parry et al., 2008). Under HTS, ATP and ADP contents decreased, indicating the blockage of photoreaction ATP synthesis. Mg-treated plants had higher ATP content, which is consistent with the findings from Busch and Ninnemann (1997). We monitored RCA activity in terms of the ratio of ATP to ADP (Carmo-Silva et al., 2015). The positive correlation between the RCA activity and the ATP/ADP ratio implied that a higher ATP/ADP ratio was closely related to the enhancement of the RCA activity (Figure 6C). HTS directly inhibited Rubisco activity, which influenced NADP<sup>+</sup> and ADP reduction. Next, electron transfer was inhibited, which led to photoinhibition (Parry et al., 2008; Carmo-Silva and Salvucci, 2011; Mathur et al., 2014). Therefore, the photosynthetic system was damaged by an increase in redundant electrons. At 25DAA, ATP, and ADP contents remained higher in Mg-treated plants than in CK plants, and ATP/ADP increased significantly, indicating that Rubisco activation was maintained through Mg application, such that light energy utilization and electron transfer were relatively stabilized during the light reaction.

## REFERENCES

- Al-Khatib, K., and Paulsen, G. M. (1990). Photosynthesis and productivity during high-temperature stress of wheat genotypes from major world regions. *Crop Sci.* 30, 1127–1132. doi: 10.2135/cropsci1990.0011183X003000050034x
- Andersson, I. (2008). Catalysis and regulation in Rubisco. *J. Exp. Bot.* 59, 1555–1568. doi: 10.1093/jxb/ern091

## CONCLUSION

The results of the present study indicate that HTS caused a decrease in Rubisco carboxylation activity which inhibited photosynthesis during the wheat senescence stage, whereas Mg application maintained Rubisco carboxylation by enhancing its activation state and stabilizing the electron transfer rate. Thus, photosynthesis was sustained by Mg application under HTS. These results suggest that Mg plays an indispensable role in sustaining photosynthesis during grain filling by improving Rubisco activation state under HTS conditions.

## DATA AVAILABILITY STATEMENT

The original contributions presented in the study are included in the article/Supplementary Material, further inquiries can be directed to the corresponding author/s.

## AUTHOR CONTRIBUTIONS

YS, JH, CS, ZT, and TD conceived and designed the experiments. YS, JH, CS, SXL, and SYL developed methodologies. LG, SYL, JH, and JG analyzed the experimental data. SYL, LG, AU, YS, and XL wrote the manuscript. SXL, LG, AU, DJ, WC, ZT, and TD revised the manuscript. All the authors contributed to the article and approved the submitted version.

## FUNDING

The National Key R&D Program of China (2018YFD0300801) and the National Natural Science Foundation of China (Grant Nos. 31471443 and 31501262) supported the study.

## ACKNOWLEDGMENTS

We acknowledge other researchers and staff for providing management and skills.

## SUPPLEMENTARY MATERIAL

The Supplementary Material for this article can be found online at: <https://www.frontiersin.org/articles/10.3389/fpls.2021.675582/full#supplementary-material>

- Arnon, D. I. (1949). Copper enzymes in isolated chloroplasts. Polyphenoloxidase in *Beta vulgaris*. *Plant Physiol.* 24, 1–15. doi: 10.1104/pp.24.1.1
- Ashraf, M., and Harris, P. J. C. (2013). Photosynthesis under stressful environments: an overview. *Photosynthetica* 51, 163–190. doi: 10.1007/s11099-013-0021-6
- Austin, R. B., Edrich, J. A., Ford, M. A., and Blackwell, R. D. (1977). The fate of the dry matter, carbohydrates and 14C Lost from the leaves and stems of wheat

- during grain filling. *Annal. Bot.* 41, 1309–1321. doi: 10.1093/oxfordjournals.aob.a085419
- Bascunan-Godoy, L., Sanhueza, C., Hernandez, C. E., Cifuentes, L., Pinto, K., Alvarez, R., et al. (2018). Nitrogen supply affects photosynthesis and photoprotective attributes during drought-induced senescence in quinoa. *Front. Plant Sci.* 9:994. doi: 10.3389/fpls.2018.00994
- Berry, A. J., and Bjorkman, O. (1980). Photosynthetic response and adaptation to temperature in higher plants. *Annu. Rev. Plant Physiol.* 31, 491–543. doi: 10.1146/annurev.pp.31.060180.002423
- Boexfontvieille, E., Daventure, M., Jossier, M., Hodges, M., Zivy, M., and Tcherkez, G. (2014). Phosphorylation pattern of Rubisco activase in *Arabidopsis* leaves. *Plant Biol.* 16:550. doi: 10.1111/plb.12100
- Bracher, A., Whitney, S. M., Hartl, F. U., and Hayer-Hartl, M. (2017). Biogenesis and metabolic maintenance of rubisco. *Annu. Rev. Plant Biol.* 68, 29–60. doi: 10.1146/annurev-arplant-043015-111633
- Busch, K., and Ninnemann, H. (1997). The controlling influence of ADP, ATP and magnesium on the activities of adenylate kinase, ATP synthase, ADP/ATP translocator and the mitochondrial respiration in plants. *Plant Sci.* 128, 85–95. doi: 10.1016/s0168-9452(97)00117-9
- Cakmak, I., and YaziCi, A. M. (2010). Magnesium: a forgotten element in crop production. *Better Crops Plant Food* 94, 23–25.
- Carmo-Silva, A. E., and Salvucci, M. E. (2011). The activity of Rubisco's molecular chaperone, Rubisco activase, in leaf extracts. *Photosynth. Res.* 108, 143–155. doi: 10.1007/s1120-011-9667-8
- Carmo-Silva, A. E., and Salvucci, M. E. (2012). The temperature response of CO<sub>2</sub> assimilation, photochemical activities and Rubisco activation in *Camelina sativa*, a potential bioenergy crop with limited capacity for acclimation to heat stress. *Planta* 236, 1433–1445. doi: 10.1007/s00425-012-1691-1
- Carmo-Silva, E., Scales, J. C., Madgwick, P. J., and Parry, M. A. (2015). Optimizing R ubisco and its regulation for greater resource use efficiency. *Plant Cell Environ.* 38, 1817–1832. doi: 10.1111/pce.12425
- Chaudhuri, K. M., Dutta, P., and Das, S. (2017). Influence of homobrassinolide on photosynthetic traits during mid-grain filling stage and its impact on yield of wheat cultivars. *J. Agricul. Phys.* 17, 173–182.
- Chen, Z. C., Peng, W. T., Li, J., and Liao, H. (2018). Functional dissection and transport mechanism of magnesium in plants. *Semin. Cell Dev. Biol.* 74, 142–152. doi: 10.1016/j.semdb.2017.08.005
- Cheng, L., and Fuchigami, L. H. (2000). Rubisco activation state decreases with increasing nitrogen content in apple leaves. *J. Exp. Bot.* 51, 1687–1694. doi: 10.1093/jexbot/51.351.1687
- Choi, B. Y., and Roh, K. S. (2003). UV-B radiation affects chlorophyll and activation of rubisco by rubisco activase in *Canavalia ensiformis* L. leaves. *J. Plant Biol.* 46:117. doi: 10.1007/bf03030440
- Degen, G. E., Orr, D. J., and Carmo-Silva, E. (2021). Heat-induced changes in the abundance of wheat Rubisco activase isoforms. *New Phytol.* 229, 1298–1311. doi: 10.1111/nph.16937
- Degen, G. E., Worrall, D., and Carmo-Silva, E. (2020). An isoleucine residue acts as a thermal and regulatory switch in wheat Rubisco activase. *Plant J.* 103, 742–751. doi: 10.1111/tpj.14766
- Demirevska-Kepova, K., and Feller, U. (2004). Heat sensitivity of Rubisco, Rubisco activase and Rubisco binding protein in higher plants. *Acta Physiol. Plant.* 26, 103–114. doi: 10.1007/s11738-004-0050-7
- Djanaguiraman, M., Narayanan, S., Erdayani, E., and Prasad, P. V. V. (2020). Effects of high temperature stress during anthesis and grain filling periods on photosynthesis, lipids and grain yield in wheat. *BMC Plant Biol.* 20:268. doi: 10.1186/s12870-020-02479-0
- Farooq, M., Bramley, H., Palta, J. A., and Siddique, K. H. M. (2011). Heat stress in wheat during reproductive and grain-filling phases. *Cri. Rev. Plant Sci.* 30, 491–507. doi: 10.1080/07352689.2011.615687
- Ferguson, J. N., McAusland, L., Smith, K. E., Price, A. H., Wilson, Z. A., and Murchie, E. H. (2020). Rapid temperature responses of photosystem II efficiency forecast genotypic variation in rice vegetative heat tolerance. *Plant J.* 104, 839–855. doi: 10.1111/tpj.14956
- Gao, J., Wang, F., Sun, J., Tian, Z., Hu, H., Jiang, S., et al. (2018). Enhanced Rubisco activation associated with maintenance of electron transport alleviates inhibition of photosynthesis under low nitrogen conditions in winter wheat seedlings. *J. Exp. Bot.* 69, 5477–5488.
- Genty, B., Briantais, J.-M., and Baker, N. R. (1989). The relationship between the quantum yield of photosynthetic electron transport and quenching of chlorophyll fluorescence. *Biochim. Biophys. Acta (BBA) Gen. Sub.* 990, 87–92. doi: 10.1016/s0304-4165(89)80016-9
- Gerendás, J., and Führs, H. (2013). The significance of magnesium for crop quality. *Plant Soil* 368, 101–128. doi: 10.1007/s11104-012-1555-2
- Gibson, L., and Paulsen, G. (1999). Yield components of wheat grown under high temperature stress during reproductive growth. *Crop Sci.* 39, 1841–1846. doi: 10.2135/cropsci1999.3961841x
- Greer, D. H., and Weedon, M. M. (2012). Modelling photosynthetic responses to temperature of grapevine (*Vitis vinifera* cv. Semillon) leaves on vines grown in a hot climate. *Plant Cell Environ.* 35, 1050–1064. doi: 10.1111/j.1365-3040.2011.02471.x
- Gregersen, P. L., Foyer, C. H., and Krupinska, K. (2014). *Photosynthesis and Leaf Senescence as Determinants of Plant Productivity: Biotechnological Approaches to Barley Improvement*. Berlin: Springer, 113–138.
- Grzebisz, W. (2013). Crop response to magnesium fertilization as affected by nitrogen supply. *Plant Soil* 368, 23–39. doi: 10.1007/s11104-012-1574-z
- Hasanah, Y. S. M. (2018). Role of elicitors in chlorophyll content and stomatal density of soybean cultivars by foliar application. *J. Agron.* 17, 112–117. doi: 10.3923/ja.2018.112.117
- Hazra, S., Henderson, J. N., Liles, K., Hilton, M. T., and Wachter, R. M. (2015). Regulation of ribulose-1,5-bisphosphate carboxylase/oxygenase (rubisco) activase: product inhibition, cooperativity, and magnesium activation. *J. Biol. Chem.* 290, 24222–24236. doi: 10.1074/jbc.M115.651745
- Hortensteiner, S., and Feller, U. (2002). Nitrogen metabolism and remobilization during senescence. *J. Exp. Bot.* 53, 927–937. doi: 10.1093/jexbot/53.370.927
- Huebner, F. R., and Bietz, J. A. (1988). Quantitative variation among gliadins of wheats grown in different environments. *Cereal Chem.* 65, 362–366.
- Imai, K., Suzuki, Y., Mae, T., and Makino, A. (2008). Changes in the synthesis of Rubisco in rice leaves in relation to senescence and N influx. *Annal. Bot.* 101, 135–144. doi: 10.1093/aob/mcm270
- IPCC (2020). *Special Report on Global Warming of 1.5°C*. Cambridge: Cambridge University Press.
- Jahan, M. S., Wang, Y., Shu, S., Zhong, M., Chen, Z., Wu, J., et al. (2019). Exogenous salicylic acid increases the heat tolerance in Tomato (*Solanum lycopersicum* L.) by enhancing photosynthesis efficiency and improving antioxidant defense system through scavenging of reactive oxygen species. *Sci. Horticult.* 247, 421–429. doi: 10.1016/j.scienta.2018.12.047
- Jones, J. B., and Wolf, B. (1991). *Plant Analysis Handbook: A Practical Sampling, Preparation, Analysis, and Interpretation Guide*. Athens, GA: Micro-Macro Publishing, Inc.
- Karley, A. J., and White, P. J. (2009). Moving cationic minerals to edible tissues: potassium, magnesium, calcium. *Curr. Opin. Plant Biol.* 12, 291–298. doi: 10.1016/j.pbi.2009.04.013
- Khan, M. A., Shirazi, M. U., Shereen, A., Ali, M., Asma, B. H., Jilani, N. S., et al. (2020). Agronomical and physiological perspectives for identification of wheat genotypes for high temperature tolerance. *Pakist. J. Bot.* 52, 1973–1980. doi: 10.30848/Pjb2020-6(12)
- Kramer, D. M., Johnson, G., Kiirats, O., and Edwards, G. E. J. P. r. (2004). New fluorescence parameters for the determination of Q A redox state and excitation energy fluxes. *Photosynth. Res.* 79:209. doi: 10.1023/b:pres.0000015391.99477.0d
- Kumar, R. R., Goswami, S., Dubey, K., Singh, K., Singh, J. P., Kumar, A., et al. (2019). RuBisCo activase—a catalytic chaperone involved in modulating the RuBisCo activity and heat stress-tolerance in wheat. *J. Plant Biochem. Biotechnol.* 28, 63–75. doi: 10.1007/s13562-018-0463-9
- Kurek, I., Chang, T. K., Bertain, S. M., Madrigal, A., Liu, L., Lassner, M. W., et al. (2007). Enhanced thermostability of *Arabidopsis* Rubisco Activase improves photosynthesis and growth rates under moderate heat stress. *Plant Cell* 19, 3230–3241. doi: 10.1105/tpc.107.054171
- Kuriata, A. M., Chakraborty, M., Henderson, J. N., Hazra, S., Serban, A. J., Pham, T. V., et al. (2014). ATP and magnesium promote cotton short-form ribulose-1, 5-bisphosphate carboxylase/oxygenase (Rubisco) activase hexamer formation at low micromolar concentrations. *Biochemistry* 53, 7232–7246. doi: 10.1021/bi500968h

- Laing, W., Greer, D., Sun, O., Beets, P., Lowe, A., and Payn, T. (2000). Physiological impacts of Mg deficiency in *Pinus radiata*: growth and photosynthesis. *New Phytol.* 146, 47–57. doi: 10.1046/j.1469-8137.2000.00616.x
- Lasa, B., Frechilla, S., Aleu, M., González-Moro, B., Lamsfus, C., and Aparicio-Tejo, P. (2000). Effects of low and high levels of magnesium on the response of sunflower plants grown with ammonium and nitrate. *Plant Soil* 225, 167–174.
- Law, R. D., and Craftsbrandner, S. J. (1999). Inhibition and acclimation of photosynthesis to heat stress is closely correlated with activation of ribulose-1,5-bisphosphate carboxylase/oxygenase. *Plant Physiol.* 120, 173–181. doi: 10.1104/pp.120.1.173
- Lesk, C., Rowhani, P., and Ramankutty, N. (2016). Influence of extreme weather disasters on global crop production. *Nature* 529, 84–87. doi: 10.1038/nature16467
- Li, S., Wang, C., Chang, X., and Jing, R. (2012). Genetic dissection of developmental behavior of grain weight in wheat under diverse temperature and water regimes. *Genetica* 140, 393–405. doi: 10.1007/s10709-012-9688-z
- Li, Y., Gao, Y. X., Xu, X. M., Shen, Q. R., and Guo, S. W. (2009). Light-saturated photosynthetic rate in high-nitrogen rice (*Oryza sativa* L.) leaves is related to chloroplastic CO<sub>2</sub> concentration. *J. Exp. Bot.* 60, 2351–2360. doi: 10.1093/jxb/erp127
- Liang, C., Xiao, W., Hao, H., Xiaoqing, L., Chao, L., Lei, Z., et al. (2008). Effect of Mg<sup>2+</sup> on the structure and function of ribulose-1, 5-bisphosphate carboxylase/oxygenase. *Biol. Trace Elem. Res.* 121, 249–257.
- Lobo, A. K. M., Orr, D. J., Gutierrez, M. O., Andralojc, P. J., Sparks, C., Parry, M. A. J., et al. (2019). Overexpression of calpase decreases rubisco abundance and grain yield in wheat. *Plant Physiol.* 181, 471–479. doi: 10.1104/pp.19.00693
- Long, S. P., and Bernacchi, C. J. (2003). Gas exchange measurements, what can they tell us about the underlying limitations to photosynthesis? Procedures and sources of error. *J. Exp. Bot.* 54, 2393–2401. doi: 10.1093/jxb/erg262
- Makino, A. (2003). Rubisco and nitrogen relationships in rice: leaf photosynthesis and plant growth. *Soil Sci. Plant Nutr.* 49, 319–327. doi: 10.1080/00380768.2003.10410016
- Makino, A., Mae, T., and Ohira, K. (1985). Enzymic properties of ribulose-1, 5-bisphosphate carboxylase/oxygenase purified from rice leaves. *Plant Physiol.* 79, 57–61. doi: 10.1104/pp.79.1.57
- Makunga, O., Pearman, I., Thomas, S., and Thorne, G. N. (1978). Distribution of photosynthate produced before and after anthesis in tall and semi-dwarf winter wheat, as affected by nitrogen fertilizer. *Annal. Appl. Biol.* 88, 429–437. doi: 10.1111/j.1744-7348.1978.tb00735.x
- Marschner, H. (1995). *Mineral Nutrition of Higher Plants*, 2 Edn. London: Academic Press.
- Mathur, S., Agrawal, D., and Jajoo, A. (2014). Photosynthesis: response to high temperature stress. *J. Photochem. Photobiol. B Biol.* 137, 116–126. doi: 10.1016/j.jphotobiol.2014.01.010
- Maxwell, K., and Johnson, G. N. (2000). Chlorophyll fluorescence—a practical guide. *J. Exp. Bot.* 51, 659–668. doi: 10.1093/jxb/51.345.659
- Mengutay, M., Ceylan, Y., Kutman, U. B., and Cakmak, I. (2013). Adequate magnesium nutrition mitigates adverse effects of heat stress on maize and wheat. *Plant Soil* 368, 57–72. doi: 10.1007/s11104-013-1761-6
- Miller, T. D. (1992). *Growth Stages of Wheat*. Atlanta, GA: Potash & Phosphate Institute, 76.
- Nehe, A., Misra, S., Murchie, E., Chinnathambi, K., Tyagi, B. S., and Foulkes, M. (2020). Nitrogen partitioning and remobilization in relation to leaf senescence, grain yield and protein concentration in Indian wheat cultivars. *Field Crops Res.* 251:107778. doi: 10.1016/j.fcr.2020.107778
- Parry, M. A. J. K., Alfred, J., Madgwick, P. J., Carmo-Silva, A. E., and Andralojc, P. J. (2008). Rubisco regulation: a role for inhibitors. *J. Exp. Bot.* 59, 1569–1580. doi: 10.1093/jxb/ern084
- Parry, M. A. J., Andralojc, P. J., Scales, J. C., Salvucci, M. E., Carmo-Silva, A. E., Alonso, H., et al. (2012). Rubisco activity and regulation as targets for crop improvement. *J. Exp. Bot.* 64, 717–730. doi: 10.1093/jxb/ers336
- Paulsen, G. M. (1994). “High temperature responses of crop plants,” in *Physiology and Determination of Crop Yield*, eds K. J. Boote, J. M. Bennett, T. R. Sinclair, and G. M. Paulsen (Madison, WI: ASA-CSSA-SSSA), 365–389. doi: 10.2134/1994.physiologyanddetermination.c25
- Peng, W. T., Qi, W. L., Nie, M. M., Xiao, Y. B., Liao, H., and Chen, Z. C. (2019). Magnesium supports nitrogen uptake through regulating NRT2.1/2.2 in soybean. *Plant Soil* 457, 97–111. doi: 10.1007/s11104-019-04157-z
- Perdomo, J. A., Capó-Bauçà, S., Carmo-Silva, E., and Galmés, J. (2017). Rubisco and rubisco activase play an important role in the biochemical limitations of photosynthesis in rice, wheat, and maize under high temperature and water deficit. *Front. Plant Sci.* 8:490. doi: 10.3389/fpls.2017.00490
- Plaut, Z., Butow, B. J., Blumenthal, C. S., and Wrigley, C. W. (2004). Transport of dry matter into developing wheat kernels and its contribution to grain yield under post-anthesis water deficit and elevated temperature. *Field Crops Res.* 86, 185–198. doi: 10.1016/j.fcr.2003.08.005
- Porter, J. R., and Gawith, M. (1999). Temperatures and the growth and development of wheat: a review. *Eur. J. Agron.* 10, 23–36. doi: 10.1016/s1161-0301(98)00047-1
- Portis, A. R. Jr. (2003). Rubisco activase – Rubisco’s catalytic chaperone. *Photosynth. Res.* 75, 11–27. doi: 10.1023/a:1022458108678
- Potarzycki, J. (2008). Influence of nitrogen and magnesium fertilization at the flag leaf stage of winter wheat development on the yield and grain quality. *Nawozy i Nawożenie* 32, 100–110.
- Richards, R. A. (2000). Selectable traits to increase crop photosynthesis and yield of grain crops. *J. Exp. Bot.* 51, 447–458. doi: 10.1093/jxb/51.suppl\_1.447
- Ristic, Z., Momčilović, I., Bukovnik, U., Prasad, P. V., Fu, J., DeRidder, B. P., et al. (2009). Rubisco activase and wheat productivity under heat-stress conditions. *J. Exp. Bot.* 60, 4003–4014. doi: 10.1093/jxb/erp241
- Sabater, B., and Martin, M. (2013). *Chloroplast Control of Leaf Senescence*. Dordrecht: Springer.
- Sales, C. R. G., da Silva, A. B., and Carmo-Silva, E. (2020). Measuring Rubisco activity: challenges and opportunities of NADH-linked microtiter plate-based and <sup>14</sup>C-based assays. *J. Exp. Bot.* 71, 5302–5312. doi: 10.1093/jxb/eraa289
- Salvucci, M. E., and Crafts-Brandner, S. J. (2004a). Inhibition of photosynthesis by heat stress: the activation state of Rubisco as a limiting factor in photosynthesis. *Physiol. Plant.* 120, 179–186. doi: 10.1111/j.0031-9317.2004.0173.x
- Salvucci, M. E., and Crafts-Brandner, S. J. (2004b). Relationship between the heat tolerance of photosynthesis and the thermal stability of Rubisco activase in plants from contrasting thermal environments. *Plant Physiol.* 134:1460. doi: 10.1104/pp.103.038323
- Santos, C. A., and Boiteux, L. S. (2013). Breeding biofortified cowpea lines for semi-arid tropical areas by combining higher seed protein and mineral levels. *Embr. Hort. Artig. Periód. Index. (ALICE)* 12, 6782–6789. doi: 10.4238/2013.December.16.4
- Scafaro, A. P., Bautsoens, N., den Boer, B., Van Rie, J., and Gallé, A. (2019). A conserved sequence from heat-adapted species improves Rubisco activase thermostability in wheat. *Plant Physiol.* 181, 43–54. doi: 10.1104/pp.19.00425
- Scafaro, A. P., Galle, A., Van Rie, J., Carmo-Silva, E., Salvucci, M. E., and Atwell, B. J. (2016). Heat tolerance in a wild *Oryza* species is attributed to maintenance of Rubisco activation by a thermally stable Rubisco activase ortholog. *New Phytol.* 211, 899–911. doi: 10.1111/nph.13963
- Scaligero, M. (2004). Inhibition of photosynthesis by heat stress: the activation state of Rubisco as a limiting factor in photosynthesis. *Physiol. Plant.* 120, 179–186. doi: 10.1111/j.0031-9317.2004.0173.x
- Shah, N. H., and Paulsen, G. M. (2003). Interaction of drought and high temperature on photosynthesis and grain-filling of wheat. *Plant Soil* 257, 219–226. doi: 10.1023/a:1026237816578
- Sharwood, R. E., Sonawane, B. V., Ghannoum, O., and Whitney, S. M. (2016). Improved analysis of C<sub>4</sub> and C<sub>3</sub> photosynthesis via refined in vitro assays of their carbon fixation biochemistry. *J. Exp. Bot.* 67, 3137–3148.
- Shen, J., Song, L., Muller, K., Hu, Y., Song, Y., Yu, W., et al. (2016). Magnesium alleviates adverse effects of lead on growth, photosynthesis, and ultrastructural alterations of *torreya grandis* seedlings. *Front. Plant Sci.* 7:1819. doi: 10.3389/fpls.2016.01819
- Shivhare, D., and Mueller-Cajar, O. (2017). In vitro characterization of thermostable CAM Rubisco activase reveals a Rubisco interacting surface loop. *Plant Physiol.* 174, 1505–1516. doi: 10.1104/pp.17.00554
- Streusand, V., and Portis, A. R. (1987). Rubisco activase mediates ATP-dependent activation of ribulose bisphosphate carboxylase. *Plant Physiol.* 85, 152–154. doi: 10.1104/pp.85.1.152

- Szulc, P. (2010). Response of maize hybrid (*Zea mays* L.), stay-green type to fertilization with nitrogen, sulphur, and magnesium. Part I. Yields and chemical composition. *Acta Scient. Polon. Agricult.* 10, 29–40.
- Tahir, I. S. A., and Nakata, N. (2005). Remobilization of nitrogen and carbohydrate from stems of bread wheat in response to heat stress during grain filling. *J. Agron. Crop Sci.* 191, 106–115. doi: 10.1111/j.1439-037x.2004.00127.x
- Tanoi, K., and Kobayashi, N. I. (2015). Leaf senescence by magnesium deficiency. *Plants* 4, 756–772. doi: 10.3390/plants4040756
- Tcherkez, G. (2013). Modelling the reaction mechanism of ribulose-1, 5-bisphosphate carboxylase/oxygenase and consequences for kinetic parameters. *Plant Cell Environ.* 36, 1586–1596. doi: 10.1111/pce.12066
- Uchida, R. (2000). Essential nutrients for plant growth: nutrient functions and deficiency symptoms. *Plant Nutr. Manag. Hawaii Soils* 20, 31–55.
- Von Caemmere, S. (1985). Kinetics and activation of Rubisco and some preliminary modelling of RuP<sub>2</sub> pool sizes. *Kinet. Photosynth. Photorespir. C 3 Plants* 85, 46–48.
- Wahid, A., Gelani, S., Ashraf, M., and Foolad, M. R. (2007). Heat tolerance in plants: An overview. *Environ. Exp. Bot.* 61, 199–223. doi: 10.1016/j.envexpbot.2007.05.011
- Wajid, M., Khan, M. A., Shirazi, M. U., Summiya, F., and Saba, M. (2018). Seed priming induced high temperature tolerance in wheat by regulating germination metabolism and physio-biochemical properties. *Int. J. Agricult. Biol.* 20, 2140–2148.
- Wang, J., Leister, D., and Bolle, C. (2015). Photosynthetic lesions can trigger accelerated senescence in *Arabidopsis thaliana*. *J. Exp. Bot.* 66, 6891–6903. doi: 10.1093/jxb/erv393
- Waraich, E. A., Ahmad, R., Saifullah, U., Ashraf, M. Y., and Ehsanullah. (2011). Role of mineral nutrition in alleviation of drought stress in plants. *Austr. J. Crop Sci.* 5, 764–777.
- Weis, E. (1981). Reversible effects of high, sublethal temperatures on light-induced light scattering changes and electrochromic pigment absorption shift in spinach leaves. *Zeitschr. Pflanzenphysiol.* 101, 169–178. doi: 10.1016/s0044-328x(81)80051-7
- Weston, D. J., and Bauerle, W. L. J. T. P. (2007). Inhibition and acclimation of C3 photosynthesis to moderate heat: a perspective from thermally contrasting genotypes of *Acer rubrum* (red maple). *Tree Physiol.* 27, 1083–1092. doi: 10.1093/treephys/27.8.1083
- Yamori, W., Hikosaka, K., and Way, D. A. (2013). Temperature response of photosynthesis in C3, C4, and CAM plants: temperature acclimation and temperature adaptation. *Photosynth. Res.* 119, 101–117. doi: 10.1007/s11120-013-9874-6
- Yang, Z. J., Sinclair, T. R., Zhu, M., Messina, C. D., Cooper, M., and Hammer, G. L. (2012). Temperature effect on transpiration response of maize plants to vapour pressure deficit. *Environ. Exp. Bot.* 78, 157–162. doi: 10.1016/j.envexpbot.2011.12.034

**Conflict of Interest:** The authors declare that the research was conducted in the absence of any commercial or financial relationships that could be construed as a potential conflict of interest.

Copyright © 2021 Shao, Li, Gao, Sun, Hu, Ullah, Gao, Li, Liu, Jiang, Cao, Tian and Dai. This is an open-access article distributed under the terms of the Creative Commons Attribution License (CC BY). The use, distribution or reproduction in other forums is permitted, provided the original author(s) and the copyright owner(s) are credited and that the original publication in this journal is cited, in accordance with accepted academic practice. No use, distribution or reproduction is permitted which does not comply with these terms.